

Correspondence

Cramér–Rao Lower Bounds for Subcarrier SNR Estimates Over Multicarrier Channels

Faouzi Bellili, Alex Stéphenne, and Sofiène Affes

Abstract—Considering orthogonal frequency-division multiplexing transmissions, analytical expressions for the Cramér–Rao lower bounds for the subcarrier signal-to-noise ratio (SNR) estimates are derived. The transmitted signal is assumed to be corrupted by additive white Gaussian noise on the different subcarriers. The channel is assumed to be slowly time-varying over the observation interval, so that it can be assumed constant. It will be shown that the achievable performance on subcarrier SNR estimation can be significantly improved by exploiting the mutual information (the same experienced noise power) between the different tones.

Index Terms—Cramér–Rao lower bounds, estimation, multicarrier, quadrature amplitude modulation (QAM), signal-to-noise ratio (SNR).

I. INTRODUCTION

Not very much information is available from the open literature on signal-to-noise ratio (SNR) subcarrier estimation, despite the fact that it is often a requirement for many applications of multicarrier transmissions. In fact, SNR estimates are often required for bit allocation algorithms, where they are usually computed at the receiver then sent back to the transmitter using feedback. Among these bit allocation strategies, we can cite the incremental allocation, the channel capacity approximation-allocation, and the probability of error-based allocation [2]. Furthermore, accurate subcarrier SNR estimates are also required for the adaptive bit loading strategies. In fact, many of the multicarrier modulation systems, especially the wireless ones [3], use conventional multicarrier modulation, which employs the same constellation size on all the subcarriers. However, the performance of these systems is typically limited by the subcarriers with poorest error performance. One solution to this problem is to perform adaptive “bit loading” where the constellation size varies from one subcarrier to another according to the SNR values measured over the subcarriers. In extreme situations, the subcarriers experiencing poor SNR values can be *nulled* or “turned off.”

Roughly speaking, depending on whether or not the transmitted symbols are assumed to be perfectly or partially known to the receiver, SNR estimators can be categorized, respectively, into the following major

categories: non-data-aided (NDA) and data-aided (DA) estimators. In fact, unlike DA SNR estimators which assume an *a priori* knowledge of all or only a subset of the transmitted symbols, NDA estimators base the estimation process only on the received samples and do not therefore impinge on the whole throughput of the system.

In parameter estimation, the performance of any unbiased estimator is usually statistically assessed by computing and plotting its variance as a function of the true value of the considered parameter, using Monte Carlo computer simulations. Specifically, a given unbiased SNR estimator is said to outperform another one if it has lower variance. However, a well-known common lower bound for the variance of any unbiased SNR estimator is the Cramér–Rao lower bound (CRLB), which informs about the achievable performance of SNR estimators. SNR estimates can be obtained using the magnitude of the received samples, and the corresponding estimators are referred to as envelope-based SNR estimators. More accurate SNR estimates can be obtained using the in-phase and quadrature (I/Q) components of the received samples. In this case, the corresponding estimators are called I/Q SNR estimators and the corresponding CRLBs are referred to as I/Q CRLBs.

In single-carrier transmissions over constant additive white Gaussian noise (AWGN) channels and for the linear modulation schemes, the CRLBs for the SNR estimates are already available in the literature. They are either derived in closed forms or numerically computed [4]–[7]. But they have never been addressed in the case of multicarrier transmissions when the SNR per subcarrier is considered, taking into account the mutual information (the same experienced noise power) between subcarriers. In this paper, always considering constant AWGN channels across all the subcarriers, we derive the CRLBs on the variance of the unbiased subcarrier SNR estimators. This will show how the mutual information between the different tones can improve the achievable performance of per-carrier SNR estimators, as it could be intuitively stated.

This paper is organized as follows. In Section II, we will introduce the system model used throughout. Then, in Section III, we will derive the CRLBs for the subcarrier SNR estimates. We will present in Section IV, as an example, some graphical representations of the NDA SNR estimation CRLBs for square quadrature amplitude modulation (QAM) constellation modulated signals. Lastly, conclusions are drawn in Section V.

II. SYSTEM MODEL

We consider a digital communication system broadcasting and receiving any orthogonal frequency-division multiplexed (OFDM) modulated signal over K subcarriers. One of the advantages of OFDM transmissions is to transform a wide-band selective multipath channel into K per-carrier narrow-band flat fading channels. In this paper, the i th per-carrier channel is assumed to be nonselective and slowly time-varying over the observation interval, so that its single channel-gain coefficient S_i can be supposed constant but different from one carrier to another. This is a valid assumption especially for wireless multicarrier communications [8], [9]. We assume also that the received signal, on the i th subcarrier ($i = 1, 2, \dots, K$), is AWGN-corrupted with noise power $2\sigma_i^2$. Assuming an ideal receiver with perfect synchronization, the output of the matched filter can be modelled as a complex signal as follows:

$$y_i(n) = S_i \alpha_i(n) e^{j\phi_i} + w_i(n), \quad n = 1, 2, \dots, N \quad (1)$$

Manuscript received February 09, 2009; accepted July 16, 2009. First published August 18, 2009; current version published January 13, 2010. The associate editor coordinating the review of this manuscript and approving it for publication was Prof. James Lam. This work was supported by the Cooperative Research and Development Program of NSERC, by PROMPT-Quebec, by Ericsson Canada and by a Canada Research Chair in Wireless Communications. This work was presented in part at IEEE Vehicular Technology Conference, Spring 2009.

F. Bellili and S. Affes are with INRS-EMT, Montreal, PQ H5A 1K6, Canada (e-mail: bellili@emt.inrs.ca; affes@emt.inrs.ca).

A. Stéphenne is with INRS-EMT, Montreal, PQ H5A 1K6, Canada, and with Ericsson Canada, Montreal, PQ H4P 2N2, Canada (e-mail: stephenne@ieee.org).

Color versions of one or more of the figures in this paper are available online at <http://ieeexplore.ieee.org>.

Digital Object Identifier 10.1109/TSP.2009.2030597

where, during the observation interval, $\{\alpha_i(n)\}_{n=1,2,\dots,N}$ are N transmitted symbols on the i th subcarrier ($i = 1, 2, \dots, K$). On the same tone, $\{y_i(n)\}_{n=1,2,\dots,N}$ are the corresponding N received samples and $w_i(n)$ are the additive white noise components that are modelled by complex Gaussian random variables with independent real and imaginary parts. The noise components are also assumed to be mutually independent between the different subcarriers. The parameter ϕ_i accounts for any constant phase distortion introduced by the channel. Moreover, to provide standard CRLBs, which are independent from the emission power, the constellation energy is supposed to be normalized to one, i.e., $E\{|\alpha_i(n)|^2\} = 1$.

Note that our system model stands as well when the L subcarriers experiencing the same noise power, $2\sigma^2$, are not at the beginning of the range. This is because the last $K-L$ subcarriers assumed to experience different noise powers, $\{2\sigma_i^2\}_{i=L+1}^K$, can always be split into any two mutually exclusive subsets, each containing m and n different tones (i.e., $K-L = m+n$), where one subset is at the beginning and the other one is at the end of the range in order to have the L subcarriers, experiencing the same noise power, lying in the middle of the range. But in this case, one can always, without loss of generality, rearrange the different tones in order to have the L tones experiencing the same noise power at the beginning of the range as assumed in this paper just for the sake of simplicity.¹

Now considering the received samples on all the subcarriers, the received signal can be more conveniently written in the following ($N \times K$) matrix form:

$$[\mathbf{Y}]_{n,i} = y_i(n). \quad (2)$$

In this paper, we will consider the most general case where we will assume that we do not have any *a priori* information about the dependence that may exist between the channel coefficients $\{S_i\}_{i=1,2,\dots,K}$ across the different subcarriers. Consequently, we suppose that the only available information is $S_i \neq S_j$ for $i \neq j$. On the other hand, without loss of generality,² we will assume that only the first L subcarriers experience the same noise power $2\sigma^2$ and the remaining $K-L$ subcarriers experience different noise powers $\{2\sigma_i^2\}_{i=L+1,L+2,\dots,K}$.

The subcarrier SNRs that we wish to estimate, using the N received samples on each subcarrier, are given by:³

$$\rho_i = \begin{cases} \frac{S_i^2}{2\sigma^2}, & i = 1, 2, \dots, L \\ \frac{S_i^2}{2\sigma_i^2}, & i = L+1, L+2, \dots, K \end{cases}. \quad (3)$$

From (3), we see that there are $2K-L+1$ parameters, σ^2 , $\{S_i\}_{i=1,2,\dots,K}$, and $\{\sigma_i\}_{i=L+1,L+2,\dots,K}$, which are involved in the expressions of the subcarrier SNRs and therefore in the derivation of the CRLBs for their corresponding estimates. Thus, we define the following parameter vector:

$$\boldsymbol{\theta} = [S_1, S_2, S_3, \dots, S_L, \sigma^2, S_{L+1}, \sigma_{L+1}^2, S_{L+2}, \sigma_{L+2}^2, \dots, S_K, \sigma_K^2]^T \quad (4)$$

$$= [\theta_1, \theta_2, \dots, \theta_{2K-L+1}]^T. \quad (5)$$

¹Note that the position of the subcarriers experiencing the same noise power can be obtained by simply estimating the noise power on each tone using, for instance, the M_2M_4 algorithm [10].

²In practice, usually the noise power would be the same over all the subcarriers, and therefore one should take $L = K$.

³Recall that $E\{|\alpha_i(n)|^2\} = 1$ and hence does not appear in the SNR expression.

On the other hand, since for a clearer interpretation, we usually use the decibel scale, we will consider the parameter transformation $g_i(\boldsymbol{\theta}) = 10 \log_{10}(\rho_i)$ given by

$$g_i(\boldsymbol{\theta}) = \begin{cases} 10 \log_{10} \left(\frac{S_i^2}{2\sigma^2} \right), & \text{for } i = 1, 2, \dots, L \\ 10 \log_{10} \left(\frac{S_i^2}{2\sigma_i^2} \right), & \text{for } i = L+1, \dots, K \end{cases} \quad (6)$$

which can be conveniently rewritten in the following K -dimensional parameter transformation:

$$\mathbf{g}(\boldsymbol{\theta}) = [g_1(\boldsymbol{\theta}), g_2(\boldsymbol{\theta}), g_3(\boldsymbol{\theta}), \dots, g_K(\boldsymbol{\theta})]. \quad (7)$$

III. DERIVATION OF THE SUBCARRIER SNR CRLBS

In this section, based on the foregoing assumptions, we will derive the Cramér–Rao bounds of the subcarrier SNR estimates when the received signal is AWGN-corrupted and the noise components are uncorrelated between subcarriers. Therefore, we denote by $P[\mathbf{Y}; \boldsymbol{\theta}]$ the probability density function of \mathbf{Y} parameterized by $\boldsymbol{\theta}$. As shown in [11], the covariance matrix $\mathbf{C}_{\hat{\rho}}$ of any unbiased subcarrier SNR estimator $\hat{\rho} = [\hat{\rho}_1, \hat{\rho}_1, \dots, \hat{\rho}_K]$, where $\hat{\rho}_i$ is an estimate of ρ_i for $i = 1, 2, \dots, K$, satisfies

$$\mathbf{C}_{\hat{\rho}} - \frac{\partial \mathbf{g}(\boldsymbol{\theta})}{\partial \boldsymbol{\theta}} \mathbf{I}^{-1}(\boldsymbol{\theta}) \frac{\partial \mathbf{g}(\boldsymbol{\theta})^T}{\partial \boldsymbol{\theta}} \geq \mathbf{0} \quad (8)$$

where “ $\geq \mathbf{0}$ ” means that the matrix is positive semidefinite and $\mathbf{I}(\boldsymbol{\theta})$ is the Fisher information matrix (FIM), which is given by

$$[\mathbf{I}(\boldsymbol{\theta})]_{ij} = -E_{\mathbf{Y}} \left\{ \frac{\partial^2 \ln P[\mathbf{Y}; \boldsymbol{\theta}]}{\partial \theta_i \partial \theta_j} \right\} \quad (9)$$

and $\partial \mathbf{g}(\boldsymbol{\theta}) / \partial \boldsymbol{\theta}$ is the ($K \times (2K-L+1)$) Jacobian matrix [11] given by:

$$\left[\frac{\partial \mathbf{g}(\boldsymbol{\theta})}{\partial \boldsymbol{\theta}} \right]_{ij} = \frac{\partial g_i(\boldsymbol{\theta})}{\partial \theta_j}. \quad (10)$$

In (9), $E_{\mathbf{Y}}\{\cdot\}$ simply returns the expected value with respect to \mathbf{Y} . Now, using (4)–(7) and (10), it can be seen that $\partial \mathbf{g}(\boldsymbol{\theta}) / \partial \boldsymbol{\theta}$ reduces simply to the following block matrix:

$$\frac{\partial \mathbf{g}(\boldsymbol{\theta})}{\partial \boldsymbol{\theta}} = \begin{pmatrix} \mathbf{G}_1 & \mathbf{0}_{p_1 \times q_1} \\ \mathbf{0}_{p_2 \times q_2} & \mathbf{G}_2 \end{pmatrix} \quad (11)$$

where, for any integers p and q , $\mathbf{0}_{p \times q}$ denotes a ($p \times q$) matrix of zero elements, $p_1 = K-L$, $q_1 = L+1$, $p_2 = L$, $q_2 = K-L$, and \mathbf{G}_1 and \mathbf{G}_2 are given as follows:

$$\mathbf{G}_1 = \begin{pmatrix} \frac{\partial g_1(\boldsymbol{\theta})}{\partial S_1} & 0 & \dots & 0 & \frac{\partial g_1(\boldsymbol{\theta})}{\partial \sigma^2} \\ 0 & \ddots & \ddots & \vdots & \vdots \\ \vdots & \ddots & \ddots & 0 & \vdots \\ 0 & \dots & 0 & \frac{\partial g_L(\boldsymbol{\theta})}{\partial S_L} & \frac{\partial g_L(\boldsymbol{\theta})}{\partial \sigma^2} \end{pmatrix}$$

$$\mathbf{G}_2 = \begin{pmatrix} \frac{\partial g_{L+1}(\boldsymbol{\theta})}{\partial \sigma_{L+1}^2} & \mathbf{0}_{1 \times 2} & \dots & \mathbf{0}_{1 \times 2} \\ \mathbf{0}_{1 \times 2} & \ddots & \ddots & \vdots \\ \vdots & \ddots & \ddots & \mathbf{0}_{1 \times 2} \\ \mathbf{0}_{1 \times 2} & \dots & \mathbf{0}_{1 \times 2} & \frac{\partial g_K(\boldsymbol{\theta})}{\partial \sigma_K^2} \end{pmatrix} \quad (12)$$

where it should be noted that \mathbf{G}_2 is also a diagonal block matrix with $\boldsymbol{\theta}^*$ being given by

$$\boldsymbol{\theta}^i = \begin{cases} [S_i, \sigma^2], & \text{for } i = 1, 2, \dots, L \\ [S_i, \sigma_i^2], & \text{for } i = L+1, L+2, \dots, K \end{cases} \quad (13)$$

Next, we will derive the FIM elements given by (9). In fact, since the transmitted symbols are independent and corrupted by independent

noise components between the subcarriers, the probability of the received matrix \mathbf{Y} parameterized by $\boldsymbol{\theta}$ is given by

$$P[\mathbf{Y}; \boldsymbol{\theta}] = \prod_{i=1}^K P[\mathbf{y}_i; \boldsymbol{\theta}^i] \quad (14)$$

where $\boldsymbol{\theta}^i$ is given by (13) and \mathbf{y}_i is a vector that contains the received samples on the i th subcarrier:

$$\mathbf{y}_i = [y_i(1), y_i(2), \dots, y_i(N)], \quad i = 1, 2, \dots, K. \quad (15)$$

Consequently, the log-likelihood function for the NK received samples is

$$\ln(P[\mathbf{Y}; \boldsymbol{\theta}]) = \sum_{i=1}^K \ln(P[\mathbf{y}_i; \boldsymbol{\theta}^i]). \quad (16)$$

Moreover, for ease of notation, from now on, we will use the following:

$$\begin{aligned} c &= -E \left\{ \frac{\partial^2 \ln(P[\mathbf{Y}; \boldsymbol{\theta}])}{\partial \sigma^2} \right\}, \\ a_i &= -E \left\{ \frac{\partial^2 \ln(P[\mathbf{y}_i; \boldsymbol{\theta}^i])}{\partial S_i^2} \right\}, \quad 1 \leq i \leq K \\ b_i &= \begin{cases} -E \left\{ \frac{\partial^2 \ln(P[\mathbf{y}_i; \boldsymbol{\theta}^i])}{\partial S_i \partial \sigma^2} \right\}, & 1 \leq i \leq L \\ -E \left\{ \frac{\partial^2 \ln(P[\mathbf{y}_i; \boldsymbol{\theta}^i])}{\partial S_i \partial \sigma_i^2} \right\}, & L+1 \leq i \leq K \end{cases} \\ d_i &= \begin{cases} -E \left\{ \frac{\partial^2 \ln(P[\mathbf{y}_i; \boldsymbol{\theta}^i])}{\partial \sigma^2} \right\}, & 1 \leq i \leq L \\ -E \left\{ \frac{\partial^2 \ln(P[\mathbf{y}_i; \boldsymbol{\theta}^i])}{\partial \sigma_i^2} \right\}, & L+1 \leq i \leq K \end{cases}. \end{aligned} \quad (17)$$

It should be noted that $\{a_i\}_{i=1,2,\dots,K}$, $\{b_i\}_{i=1,2,\dots,K}$, and $\{d_i\}_{i=1,2,\dots,K}$ are the elements of the FIM that would be obtained if we were to consider on the $\{i$ th $\}_{i=1,2,\dots,K}$ subcarrier the corresponding received N samples $\{y_i(n)\}_{n=1,2,\dots,N}$ as a sequence transmitted by a traditional single-carrier system. It is also worth noting that, at this stage, we have

$$c = \sum_{i=1}^L d_i. \quad (18)$$

On the other hand, using (9) and (16), it can be shown that the FIM is also a block matrix⁴ given by

$$\mathbf{I}(\boldsymbol{\theta}) = \begin{pmatrix} \mathbf{I}_1 & \mathbf{0}_{p_3 \times q_3} \\ \mathbf{0}_{p_3 \times q_3}^T & \mathbf{I}_2 \end{pmatrix} \quad (19)$$

where $p_3 = L+1$, $q_3 = 2(K-L)$, and \mathbf{I}_1 and \mathbf{I}_2 are given by

$$\begin{aligned} \mathbf{I}_1 &= \begin{pmatrix} a_1 & 0 & 0 & \cdots & 0 & b_1 \\ 0 & a_2 & 0 & \cdots & 0 & b_2 \\ 0 & 0 & \ddots & \ddots & \vdots & \vdots \\ \vdots & \vdots & \ddots & \ddots & 0 & \vdots \\ 0 & 0 & \cdots & 0 & a_L & b_L \\ b_1 & b_2 & \cdots & \cdots & b_L & c \end{pmatrix} \\ \mathbf{I}_2 &= \begin{pmatrix} \mathbf{J}_{L+1}(\boldsymbol{\theta}^{L+1}) & \mathbf{0}_{2 \times 2} & \cdots & \mathbf{0}_{2 \times 2} \\ \mathbf{0}_{2 \times 2} & \ddots & \ddots & \vdots \\ \vdots & \ddots & \ddots & \mathbf{0}_{2 \times 2} \\ \mathbf{0}_{2 \times 2} & \cdots & \mathbf{0}_{2 \times 2} & \mathbf{J}_K(\boldsymbol{\theta}^K) \end{pmatrix} \end{aligned} \quad (20)$$

⁴Note here that this block structure for the FIM was also obtained with the CRLB for direction-of-arrival estimates in [12] due to the presence of decoupled parameters. Here, the decoupled parameters are $\boldsymbol{\alpha}_1 = [\theta_1, \theta_2, \dots, \theta_{L+1}]$ and $\boldsymbol{\alpha}_2 = [\theta_{L+2}, \theta_{L+3}, \dots, \theta_K]$, where $\boldsymbol{\theta} = [\boldsymbol{\alpha}_1, \boldsymbol{\alpha}_2]^T$.

where it should be noted again that \mathbf{I}_2 is also a block matrix with $\mathbf{J}_i(\boldsymbol{\theta}^i)$ being simply given by

$$\mathbf{J}_i(\boldsymbol{\theta}^i) = \begin{pmatrix} a_i & b_i \\ b_i & d_i \end{pmatrix}, \quad \text{for } i = L+1, L+2, \dots, K \quad (21)$$

which is the (2×2) FIM that would be obtained if we were only to consider the N received samples on the i th subcarrier as a sequence transmitted by a traditional single-carrier communication system.

Finally, from (8) and using (11) and (19), the CRLB of the subcarrier SNR estimator covariance matrix $\mathbf{CRLB}(\boldsymbol{\rho})$ is given by

$$\mathbf{CRLB}(\boldsymbol{\rho}) = \begin{pmatrix} \mathcal{G}_1 \mathbf{I}_1^{-1} \mathcal{G}_1^T & \mathbf{0}_{p_4 \times q_4} \\ \mathbf{0}_{p_4 \times q_4} & \mathcal{G}_2 \mathbf{I}_2^{-1} \mathcal{G}_2^T \end{pmatrix} \quad (22)$$

where $p_4 = L$ and $q_4 = K-L$. Furthermore, since we are only interested in subcarrier SNR estimation, the CRLB for SNR estimates on the i th subcarrier $\text{CRLB}^i(\rho_i)$ is given by the i th diagonal element of the matrix $\mathbf{CRLB}(\boldsymbol{\rho})$, i.e., $\{\text{CRLB}^i(\rho_i) = [\mathbf{CRLB}(\boldsymbol{\rho})]_{ii}\}_{i=1,2,\dots,K}$. In addition, for the last $K-L$ subcarriers, which are experiencing different noise powers, it can be seen that

$$\mathcal{G}_2 \mathbf{I}_2^{-1} \mathcal{G}_2^T = \begin{pmatrix} \text{CRLB}^{L+1}(\rho_{L+1}) & 0 & \cdots & 0 \\ 0 & \ddots & \ddots & \vdots \\ \vdots & \ddots & \ddots & 0 \\ 0 & \cdots & 0 & \text{CRLB}^K(\rho_K) \end{pmatrix} \quad (23)$$

where $\text{CRLB}^i(\rho_i) = (\partial g_i(\boldsymbol{\theta}^i) / \partial \theta^i) \mathbf{J}_i^{-1}(\boldsymbol{\theta}^i) (\partial g_i(\boldsymbol{\theta}^i) / \partial \theta^i)^T$, for $L+1 \leq i \leq K$, is the CRLB for the SNR estimates that can be achieved on the i th subcarrier by receiving the same corresponding N samples (\mathbf{y}_i) as being from a traditional single-carrier system. These are well covered in the literature.

However, for the first L subcarriers, which experience the same noise power $2\sigma^2$, the matrix \mathbf{I}_1 must be inverted before being able to find the CRLBs for the corresponding SNR estimates. In fact, by denoting the i th row of \mathcal{G}_1 by \mathbf{r}_i , and taking the first L diagonal elements of the matrix $\mathbf{CRLB}(\boldsymbol{\rho})$, we get the CRLBs for the SNR estimates on the first L subcarriers as follows:

$$\text{CRLB}^i(\rho_i) = \mathbf{r}_i \mathbf{I}_1^{-1} \mathbf{r}_i^T \quad i = 1, 2, \dots, L. \quad (24)$$

Furthermore, the inverse of \mathbf{I}_1 is established as shown in (25) at the bottom of the next page. Finally, using (24) and (25) and the expression of \mathcal{G}_1 given by (12), we get the analytical expressions for the CRLBs on the variance of any unbiased subcarrier SNR estimator for the first L tones as follows:

$$\begin{aligned} \text{CRLB}^i(\rho_i) &= \frac{1}{c - \sum_{l=1}^L \frac{b_l^2}{a_l}} \left[\left(\frac{c}{a_i} - \sum_{\substack{l=1 \\ l \neq i}}^L \frac{b_l^2}{a_l a_i} \right)^2 \left(\frac{\partial g_i(\boldsymbol{\theta})}{\partial S_i} \right)^2 \right. \\ &\quad \left. - 2 \frac{b_i}{a_i} \frac{\partial^2 g_i(\boldsymbol{\theta})}{\partial S_i \partial \sigma^2} + \left(\frac{\partial g_i(\boldsymbol{\theta})}{\partial \sigma^2} \right)^2 \right]. \end{aligned} \quad (26)$$

Recall that $c = \sum_{i=1}^L d_i$ and the unknowns $\{a_i\}_{i=1,2,\dots,L}$, $\{b_i\}_{i=1,2,\dots,L}$, and $\{d_i\}_{i=1,2,\dots,L}$ are the FIM elements that can be obtained for each subcarrier over which we receive the corresponding N samples as being from a classical single-carrier system. When the channel is assumed constant over the observation interval, the analytical expressions for these unknowns have already been previously derived for different modulation types, for both DA and NDA SNR estimates. For instance, for binary and quadrature phase-shift keying (PSK) modulated signals, their expressions are derived in

[6]. The generalization of their expressions to higher order square QAM-modulated signals was also carried out in [13] and [14]. In fact, by denoting the square constellation order by $M = 2^{2p}$, it was shown that

$$a_i^{\text{NDA}} = \frac{NF(\rho_i)}{2^{p-2}\sigma^2} \quad (27)$$

$$b_i^{\text{NDA}} = \frac{NS_i[A_2 - H(\rho_i)]}{2^{p-2}\sigma^4} \quad (28)$$

$$d_i^{\text{NDA}} = \frac{N \left[2^{p-2} + \frac{S_i^2}{\sigma^2} [A_2 + G(\rho_i)] - \rho_i(4A_2 + \rho_i A_4) \right]}{2^{p-2}\sigma^4} \quad (29)$$

where

$$A_m = \sum_{k=1}^{2^{p-1}} (2k-1)^m d_p^m \quad (30)$$

$$F(\rho) = \frac{1}{\sqrt{2\pi}} \int_{-\infty}^{+\infty} \frac{f_p^2(t)}{h_p(t)} e^{-\frac{t^2}{2}} dt \quad (31)$$

$$G(\rho) = \frac{1}{\sqrt{2\pi}} \int_{-\infty}^{+\infty} \frac{g_p^2(t)}{h_p(t)} e^{-\frac{t^2}{2}} dt \quad (32)$$

$$H(\rho) = \frac{1}{\sqrt{2\pi}} \int_{-\infty}^{+\infty} \frac{f_p(t) \times g_p(t)}{h_p(t)} e^{-\frac{t^2}{2}} dt \quad (33)$$

with

$$f_p(t) = \sum_{k=1}^{2^{p-1}} e^{-(2k-1)^2 d_p^2 \rho} \times \left[(2k-1) d_p t \sinh\left((2k-1) d_p \sqrt{2\rho} t\right) - (2k-1)^2 d_p^2 \sqrt{2\rho} \cosh\left((2k-1) d_p \sqrt{2\rho} t\right) \right] \quad (34)$$

$$g_p(t) = \sum_{k=1}^{2^{p-1}} e^{-(2k-1)^2 d_p^2 \rho} \times \left[(2k-1) d_p t \sinh\left((2k-1) d_p \sqrt{2\rho} t\right) - (2k-1)^2 d_p^2 \sqrt{\frac{\rho}{2}} \cosh\left((2k-1) d_p \sqrt{2\rho} t\right) \right] \quad (35)$$

$$h_p(t) = \sum_{k=1}^{2^{p-1}} e^{-(2k-1)^2 d_p^2 \rho} \times \cosh\left((2k-1) d_p \sqrt{2\rho} t\right). \quad (36)$$

Here, $2d_p = 2^p / \sqrt{2^p \sum_{k=1}^{2^{p-1}} (2k-1)^2}$ is the intersymbol distance of a normalized-energy constellation. Therefore, for square QAM-modulated signals, the CRLBs for subcarrier SNR estimates on one of the first L subcarriers can now be directly deduced using the newly derived expression (26) as follows:

$$\text{CRLB}_{\text{NDA}}^i(\rho_i) = \frac{50 \times 2^{p-1}}{N \ln(10)^2} \left[\frac{2}{\rho_i F(\rho_i)} + \frac{(2K(\rho_i) + 1)^2}{\sum_{l=1}^L \psi_p(\rho_l)} \right], \quad i = 1, 2, \dots, L \quad (37)$$

where

$$K(\rho) = \frac{A_2 - H(\rho)}{F(\rho)} \quad (38)$$

$$\psi_p(\rho) = 2^{p-2} + 2\rho G(\rho) - 2\rho A_2 - \rho^2 A_4 - \frac{2\rho(A_2 - H(\rho))^2}{F(\rho)}. \quad (39)$$

It can be seen that (37) reveals that, compared to a traditional single-carrier system, the achievable performances are effectively improved in a multicarrier system by exploiting the mutual information. In fact, the term $\{\psi_p(\rho_l)\}_{l=1,2,\dots,L;l \neq i}$ should be interpreted as the contribution of the l th subcarrier to the improvement on the achievable performances at the considered i th tone. In fact, as shown by simulations in Fig. 1, we have $\psi_p(\rho) > 0$. Therefore, the quantity $\sum_{l=1}^L \psi_p(\rho_l)$ is strictly increasing with respect to the subcarriers number L . Consequently, as this quantity appears in the denominator of the CRLB, the achievable performances are improved by increasing L . This is also shown by simulations for different values of L in Fig. 2 in the special case of a 64-QAM modulated signal.

On the other hand, (37) shows that the CRLB is inversely proportional to the observation interval size N , and therefore it decreases by increasing N . This is hardly surprising since one more received symbol carries additional information on the experienced SNR, which improves the achievable performance. Moreover, for any observation interval size N , the CRLBs can be deduced by scaling with the factor N_1/N if they were already computed for a given observation interval size N_1 . It can also be seen from (37) that the CRLB on the i th subcarrier does not depend on the corresponding phase distortion ϕ_i introduced by the channel, as expected, since a transmitted symbol and its corresponding simply rotated received sample have the same magnitude and therefore the same power. This can also be statistically explained by the fact that the derotated received samples $\mathbf{y}_i e^{-j\phi_i}$ carry the same information quantity, since they exhibit the same probability characteristic as the original received samples \mathbf{y}_i . This is because the original and the derotated noise samples are both zero-mean AWGN samples.

Furthermore, simpler expressions for the CRLBs can be obtained for high SNR values. In fact, as can be seen from Fig. 1(a), $K(\rho)$ becomes very small in this SNR region so that it can be reasonably approximated by zero. In addition, it can be seen in Fig. 1(b) that $\psi_p(\rho)$ is almost

$$\mathbf{I}_1^{-1} = \frac{1}{c - \sum_{l=1}^L \frac{b_l^2}{a_l}} \begin{pmatrix} \frac{c}{a_1} - \sum_{\substack{l=1 \\ l \neq 1}}^L \frac{b_l^2}{a_1 a_l} & \frac{b_1 b_2}{a_1 a_2} & \dots & \frac{b_1 b_L}{a_1 a_L} & -\frac{b_1}{a_1} \\ \frac{b_2 b_1}{a_2 a_1} & \frac{c}{a_2} - \sum_{\substack{l=1 \\ l \neq 2}}^L \frac{b_l^2}{a_2 a_l} & \ddots & \vdots & -\frac{b_2}{a_2} \\ \vdots & \ddots & \ddots & \frac{b_{L-1} b_L}{a_{L-1} a_L} & \vdots \\ \frac{b_L b_1}{a_L a_1} & \dots & \frac{b_L b_{L-1}}{a_L a_{L-1}} & \frac{c}{a_L} - \sum_{\substack{l=1 \\ l \neq L}}^L \frac{b_l^2}{a_L a_l} & -\frac{b_L}{a_L} \\ -\frac{b_1}{a_1} & -\frac{b_2}{a_2} & \dots & -\frac{b_L}{a_L} & 1 \end{pmatrix} \quad (25)$$

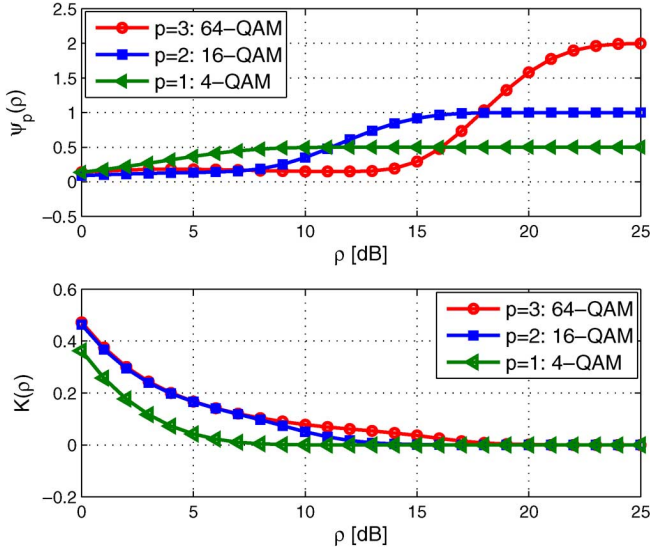


Fig. 1. Graphical representations of $K(\rho)$ and $\psi_p(\rho)$.

constant for relatively high SNR values, and it can be approximated by $\psi_p(\rho) = 2^{p-2}$. These approximations were analytically verified, but the derivations were not included due to lack of space. Hence, for high SNR values, the CRLB expression reduces simply to

$$\text{CRLB}_{\text{NDA}}^i(\rho_i) = \frac{100 \times 2^{p-1}}{N \ln(10)^2} \left(\frac{1}{\rho_i F(\rho_i)} + \frac{1}{L 2^{p-1}} \right), \quad i = 1, 2, \dots, L. \quad (40)$$

It should be mentioned again that (27)–(40) apply only for square QAM constellations, and not to quadrature-symmetric schemes in general, like PSK or amplitude PSK. Finally, it should be recalled that the CRLBs on one of the last $K - L$ subcarriers, which experience different noise powers, remain unchanged compared to the CRLBs that can be achieved over single-carrier transmissions. They can be obtained from (37) by simply replacing L by one and setting ρ_1 to ρ_i .

IV. GRAPHICAL REPRESENTATIONS AND DISCUSSIONS

In this section, we include some graphical representations of the I/Q NDA CRLBs for the subcarrier SNR estimates of square QAM-modulated signals. The I/Q NDA CRLBs for the remaining $K - L$ subcarriers were not included because they are exactly those obtained in a traditional single-carrier system. These are well covered in the literature. In this section, δ will stand for a constant SNR gap between two consecutive subcarriers, i.e., $\delta = \rho_{i+1} - \rho_i, (i = 1, 2, \dots, L - 1)$. Note that the SNR gap is chosen constant just for illustrative purposes. It should also be noted that, without loss of generality, we have illustrated simulation results only on the first subcarrier.

For QPSK- and 16-QAM-modulated signals, Fig. 3 shows the graphical representation of the CRLB using both its closed-form and approximate expressions, respectively, given by (37) and (40). It can be seen that, for relatively high SNR values, the simple expression given by (40) accurately approximates the CRLB and therefore can be used instead of (37) with much less computational cost. On the other hand, it also shows more clearly the dependence of the achievable performances on the subcarriers number L in this SNR region.

Fig. 2 depicts the behavior of the I/Q CRLBs on the first subcarrier when it is processed as if in a single-carrier system, hypothetically, or in a multicarrier system, *a priori*. We see that the CRLBs on this tone are much lower in a multicarrier system than those that can be achieved in a single-carrier system due to proper and optimal exploitation of the

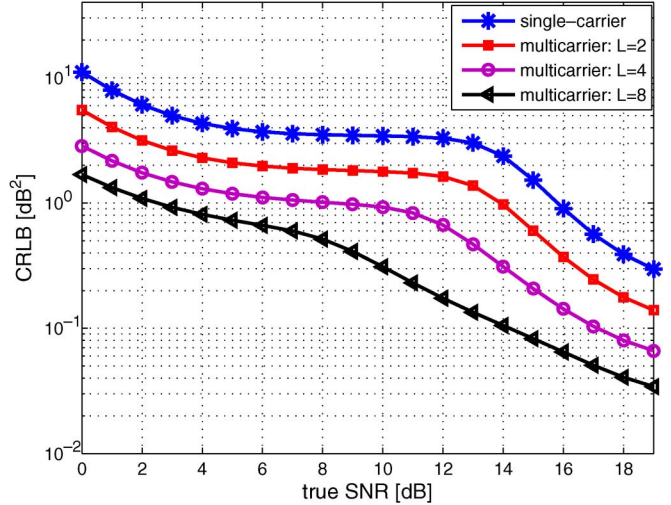


Fig. 2. CRLB of the SNR estimates on the first subcarrier for different tones $L, N = 100, 64\text{-QAM}$.

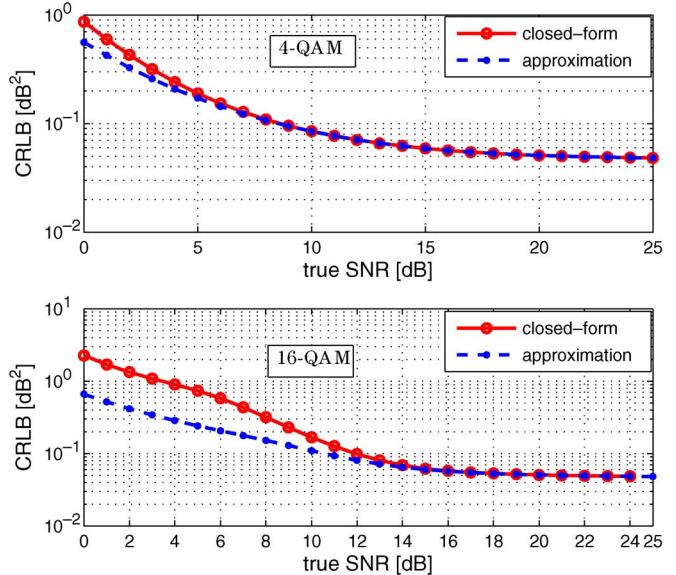


Fig. 3. CRLB of the SNR estimates on the first subcarrier and its approximation $L = 4, \delta = 1 \text{ dB}, N = 100$.

mutual information between subcarriers. These considerable improvements on the achievable performance stem from the improvements in the estimation accuracy of the noise power, which is the same on the other $L - 1$ first subcarriers. In fact, the received samples on these tones carry additional information about the common unknown noise power. However, the achievable performances of the SNR estimators on the last $K - L$ subcarriers remain unchanged. This is hardly surprising, since the noise powers are mutually different on these subcarriers and since no *a priori* knowledge is assumed about the dependence of the channel coefficients.

Lastly, Fig. 4 depicts the behavior of the CRLB with respect to the SNR gap δ . Here, positive and negative values of δ stand, respectively, for an increasing and decreasing SNR gaps between the consecutive subcarriers. The achievable performances turn out to be improved for higher δ . This is because as δ increases, the subcarriers experience higher SNRs and their contributions $\psi_p(\rho_l), l = 2, 3, \dots, L$, are higher since $\psi_p(\rho)$ is an increasing function of ρ , as seen in Fig. 1.

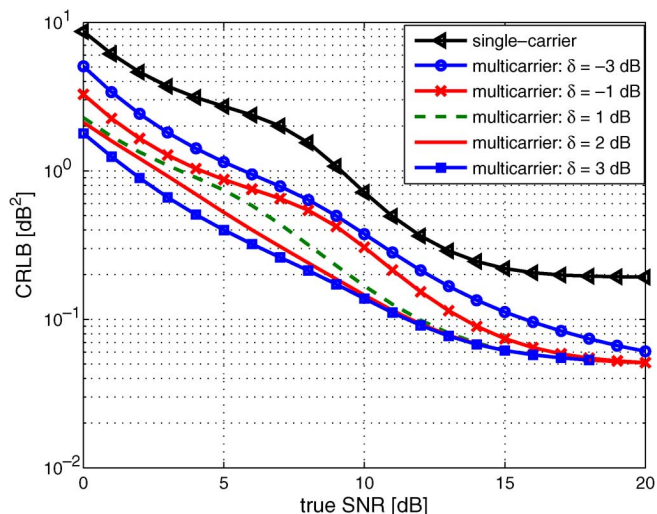


Fig. 4. CRLB of the SNR estimates on the first subcarrier for different SNR gaps, $L = 4$, $N = 100$, 16-QAM.

Therefore, as it could be intuitively stated, we see that a given subcarrier contributes better to the improvements on the SNR estimation accuracy (on another subcarrier) when it experiences higher SNR values.

Finally, we recall that the CRLB achieved on one of the remaining $K - L$ subcarriers is exactly the same that could be achieved by any subcarrier when it is processed in a single-carrier system, hypothetically. Therefore, although they were not treated in this section, the CRLBs at a given experienced SNR value ρ_i on any tone among the last $K - L$ subcarriers (experiencing different noise powers) is exactly the CRLB achieved on the first subcarrier, at the same SNR value ρ_i , when it is processed in a single-carrier system as depicted in Figs. 2 and 4.

V. CONCLUSION

Analytical expressions for the Cramér–Rao lower bounds on the variance of unbiased subcarrier SNR estimators, in multicarrier systems, are derived when the signal is corrupted by additive white Gaussian noise. The most general case was considered where no *a priori* information is assumed about the dependence that may exist between the channel coefficients across the different subcarriers. As intuitively expected, it was shown that exploiting the mutual information between the subcarriers leads to substantial improvement on the achievable performance of the unbiased subcarrier SNR estimators.

REFERENCES

- [1] F. Bellili, A. Stéphenne, and S. Affes, “Cramér–Rao bounds for SNR estimates in multicarrier transmissions,” in *Proc. IEEE VTC’09-Spring*, Barcelona, Spain, Apr. 2009.
- [2] A. M. Wyglinski, F. Labeau, and P. Kabal, “An efficient bit allocation algorithm for multicarrier modulation,” in *Proc. IEEE WCNC*, Atlanta, GA, USA, 2004, vol. 2, pp. 1194–1199.
- [3] *Wireless LAN Medium Access Control (MAC) and Physical Layer (PHY) Specifications: High-Speed Physical Layer in the 5 GHz Band*, IEEE Std. 802.11a, Nov. 1999.
- [4] P. Gao and C. Tepedelenlioglu, “SNR estimation for non-constant modulus constellations,” *IEEE Trans. Signal Process.*, vol. 53, pp. 865–870, Mar. 2005.
- [5] L. Chang, F. Wang, J. Xu, and Z. Wang, “Blind SNR estimation for arbitrary linear modulated signals,” in *Proc. IEEE Globecom*, Washington, DC, Nov. 2007, pp. 4025–4029.
- [6] N. S. Alagha, “Cramer-Rao bounds of SNR estimates for BPSK and QPSK modulated signals,” *IEEE Commun. Lett.*, vol. 5, no. 1, pp. 10–12, Jan. 2001.

- [7] W. Gappmair, “Cramér–Rao lower bound for non-data-aided SNR estimation of linear modulation schemes,” *IEEE Trans. Commun.*, vol. 56, pp. 689–693, May 2008.
- [8] J. A. C. Bingham, “Multicarrier modulation for data transmission: An idea whose time has come,” *IEEE Commun. Mag.*, pp. 5–14, May 1990.
- [9] Z. Wang and G. B. Giannakis, “Wireless multicarrier communications: Where Fourier meets Shannon,” *IEEE Signal Processing Mag.*, pp. 29–48, May 2000.
- [10] D. R. Pauluzzi and N. C. Beaulieu, “A comparison of SNR estimation techniques for the AWGN channel,” *IEEE Trans. Commun.*, vol. 48, pp. 1681–1691, Oct. 2000.
- [11] S. M. Kay, *Fundamentals of Statistical Signal Processing, Vol. 1: Estimation Theory*. Englewood Cliffs, NJ: Prentice Hall, 1993.
- [12] J. P. Delmas and H. Abeida, “Cramer-Rao bounds of DOA estimates for BPSK and QPSK modulated signals,” *IEEE Trans. Signal Process.*, vol. 54, no. 1, pp. 117–126, Jan. 2006.
- [13] F. Bellili, A. Stéphenne, and S. Affes, “Cramér–Rao lower bounds for NDA SNR estimates of square QAM modulated transmissions,” *IEEE Trans. Commun.*, Jun. 2009, accepted for publication.
- [14] F. Bellili, A. Stéphenne, and S. Affes, “Cramér–Rao bound for NDA SNR estimates of square QAM modulated signals,” in *Proc. IEEE WCNC’09*, Budapest, Hungary, April 2009.

Central Limit Theorems for Wavelet Packet Decompositions of Stationary Random Processes

Abdourrahmane M. Atto and Dominique Pastor

Abstract—This paper provides central limit theorems for the wavelet packet decomposition of stationary band-limited random processes. The asymptotic analysis is performed for the sequences of the wavelet packet coefficients returned at the nodes of any given path of the M -band wavelet packet decomposition tree. It is shown that if the input process is strictly stationary, these sequences converge in distribution to white Gaussian processes when the resolution level increases, provided that the decomposition filters satisfy a suitable property of regularity. For any given path, the variance of the limit white Gaussian process directly relates to the value of the input process power spectral density at a specific frequency.

Index Terms—Band-limited stochastic processes, spectral analysis, wavelet transforms.

I. INTRODUCTION

This paper addresses the statistical properties of the M -band discrete wavelet packet transform (M -DWPT). Specifically, an asymptotic analysis is given for the correlation structure and the distribution of the M -band wavelet packet coefficients of stationary random processes.

In [1] and [2], such a study is carried out without analyzing the role played by the path followed in the M -DWPT tree and that of the wavelet decomposition filters. In contrast, this paper emphasizes that, given a path of the M -DWPT, the sequence of the M -band wavelet packet coefficients obtained at resolution j in this path converges, in a distributional sense specified below, to a discrete white Gaussian

Manuscript received January 15, 2009; accepted August 14, 2009. First published September 09, 2009; current version published January 13, 2010. The associate editor coordinating the review of this manuscript and approving it for publication was Dr. Lucas Parra.

The authors are with the Institut TELECOM-TELECOM Bretagne, Université Européenne de Bretagne, Technopôle Brest-Iroise, 29238 Brest Cedex 3, France (e-mail: am.atto@telecom-bretagne.eu; dominique.pastor@telecom-bretagne.eu).

Digital Object Identifier 10.1109/TSP.2009.2031726